JOURNAL OF CATALYSIS 114, 321–331 (1988)

Preparation and Properties of Platinum/Ω-Zeolite Bifunctional Catalysts

BERNARD COQ,[1] FRANÇOIS FIGUERAS, AND VICTOR RAJAOFANOVA

Laboratoire de Chimie Organique Physique et Cinétique Chimique Appliquées, U.A. 418 du CNRS, Ecole Nationale Supérieure de Chimie de Montpellier, 8 rue Ecole Normale, 34075, Montpellier, Cedex, France

Received May 7, 1987; revised June 7, 1988

Platinum/Ω-zeolite catalysts have been prepared by ion exchange from Pt ammine. The main factor controlling the dispersion of the metallic phase is the vapor pressure of water inside the zeolite framework during the reduction step. By a careful check of this parameter very small platinum particles can be obtained ($d < 1$ nm). On increasing the size of the metallic particles up to 5 nm the aggregates grow in the Ω-zeolite framework by creating cavities. When additional growth occurs the particles no longer stay in the framework which suffers strong disaggregation. An initial exchange with cerium stabilizes the zeolite texture against particle growth, which then occurs at a lower platinum content. The hydroconversion of C_6 alkanes has been carried out as a probe to investigate the properties of these materials. At low platinum content it appears that the activity is not proportional to the platinum surface, thus making clear the inaccessibility of some platinum species. Accessibility is improved by a previous exchange with cerium. The presence of metallic particles inside the Ω-zeolite structure hinders strongly the diffusion of reactants. The higher the conversion level or the bulkier the reactant, the lower the activation energies (down to 10 kcal mol^{-1}). In contrast, with mechanical mixtures and poorly dispersed Pt/Ω-zeolite catalysts, activation energies of 34–38 kcal mol^{-1} for type B rearrangements have been determined. However, the selectivity of mechanical mixtures depends on the size of the zeolite particles and on the extent and nature of the microporosity. Large needles of Ω-zeolite give high selectivity for hydrocracking even at low conversion while smaller Ω particles preexchanged with cerium permit the development of a nearly pure hydroisomerization catalyst.

INTRODUCTION

Only a few catalytic studies have been devoted to synthetic Ω-zeolites (*1–4*), in spite of the large porosity reported by Flanigen (*5*). This zeolite was claimed to adsorb perfluorotributylamine, then considered as having apertures as large as 1.1 nm. However, this adsorption behavior was not confirmed in later reports (*2, 6*). Deduced from the framework proposed by Galli (*7*), the main features of the structure are the following: (i) there is a main channel along the *c* direction with a free diameter of 0.8 nm, this channel being bounded by six gmelinite cages which share their upper and lower six ring faces along the *c* axis, and (ii) the stacking of gmelinite cages gives rise to very tortuous and narrow secondary channel systems belonging to the same *c* direction; under normal conditions no communication can occur through the four- and five-membered rings separating the main and secondary channels.

A recent study of Chauvin *et al.* (*6*) on the sorptive properties of various synthetic Ω-zeolites shows that the N_2, H_2O, *n*-hexane, 1,3,5-trimethylbenzene, and 1,3,5-triisopropylbenzene uptakes are fully in line with the above-proposed framework. This unidimensional character of Ω-zeolite, and the quasi-inaccessibility of the gmelinite cage, may induce diffusional limitations not only for the reactants but also for cationic species during the preparation or the activation procedures. This last phenomenon may have two distinct drawbacks, on the one hand a pore blockage, on

[1] To whom correspondence should be addressed.

0021-9517/88 $3.00

the other hand a poor thermal stability due to exothermic effects during the burning of organic materials.

As a consequence of the above points Ω-zeolite usually exhibits good initial activity but suffers strong deactivation by coking (*1–4*). In order to study the catalytic properties of this solid more easily, a hydrogenation function, such as a Group VIII metal, can be added to lower the coke formation. The introduction into the zeolite framework of a metallic component in a very high dispersion state is easily achieved with faujasite, mordenite, and ZSM-5 zeolites, for instance. Up to now the best dispersion obtained with Ω-based catalysts is H /Pt =

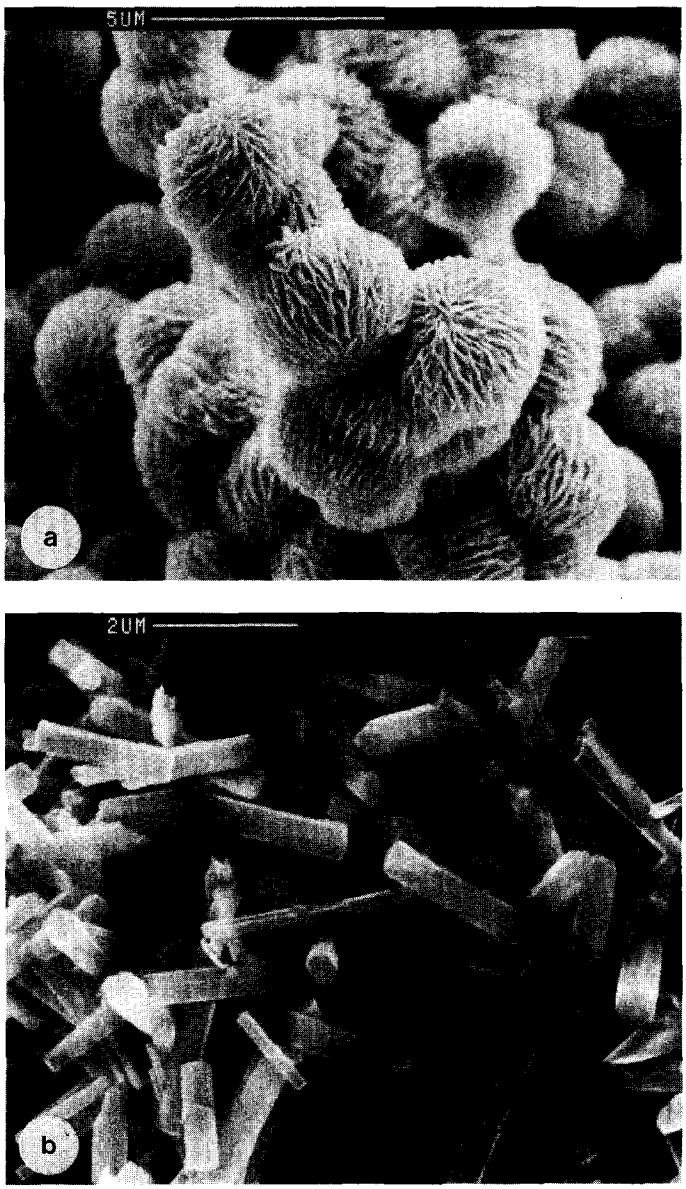

FIG. 1. Scanning electron micrographs showing the morphology of the parent zeolites SPH (a), 4I (b), and 5I (1c).

0.52 (*1*). Then the location of platinum crystallites is questionable: Are they inside or outside the crystalline framework? The conclusions drawn about the properties of Ω-zeolite might depend on the answer to this question.

The aim of the present work was twofold: first to obtain a highly dispersed Pt/Ω-zeolite catalyst, and second to study some properties of Ω-zeolites by means of the hydroisomerization of C_6 hydrocarbons.

EXPERIMENTAL

Three different samples of Ω-zeolite have been investigated in this study. The parent materials were synthesized according to patented procedures (*8*). By a change in the method of preparation (*9*), spherulitic particles (SPH), large hexagonal single crystals (4I), and polycrystalline aggregates of small particles (5I) were obtained (Fig. 1).

A rare earth exchange with $CeCl_3$ was performed on NH_4SPH to obtain the HCeSPH sample (exchange percentage, 25%). This extent of ammonium exchange is quite normal; a maximum of 50% can be reached under more severe conditions of acidity, but dealumination then occurs (*9*). All these different solids exhibit similar Si/Al ratios (SPH, 3.3; 4I, 2.9; 5I, 3.1).

The dispersion of platinum was investigated in the SPH sample in relation to the following factors: (i) the liquid to solid ratio (100 or 1000) during the exchange by $Pt(NH_3)_4^{2+}$ in competition with NH_4^+ according to a method previously described (*10*); (ii) the final temperature during the calcination step (673 to 823 K), performed during 10 h under high flow rate; (iii) the hydrogen flow rate during the reduction step (673 K); and (iv) the platinum content.

The crystallinity of the solids was determined by X-ray diffraction with a CGR Theta 60 instrument using Cu$K\alpha$ monochromated radiation. The adsorption–desorption of nitrogen at 77 K, and the chemisorption of hydrogen on platinum samples at 298 K, were performed in a conventional volumetric apparatus. The uptake of *n*-hexane at different partial pressures was determined at 298 K by a gravimetric method using a Cahn RH electrobalance connected to a flow line.

Catalytic experiments were performed

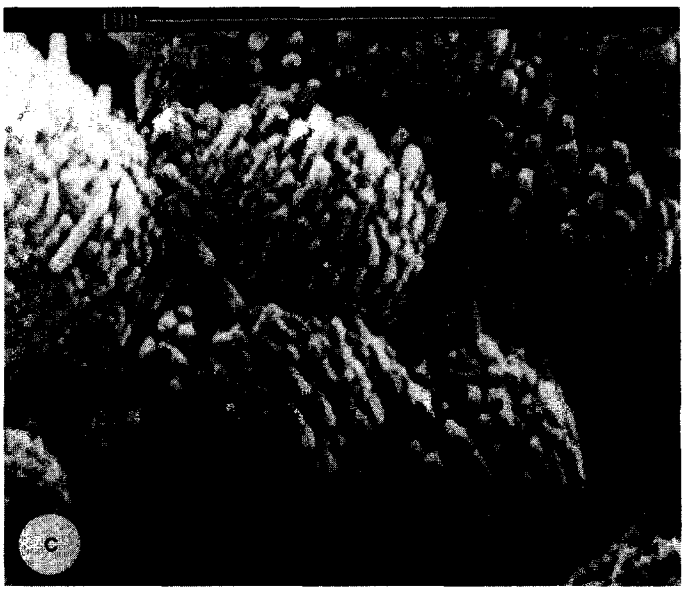

FIG. 1—*Continued.*

on platinum exchanged zeolites and on mechanical mixtures composed of the parent Ω-zeolite in protonic form and a well-dispersed Pt/Al_2O_3 catalyst (0.4 wt% Pt, H/Pt > 0.9). The conversions of *n*-hexane (*n*-H), 3-methylpentane (3MP), and methylcyclopentane (MCP) were studied in a flow microreactor (weight of catalyst, 50–100 mg) at atmospheric pressure. High-purity hydrogen (>99.99%) was used as carrier gas. The partial pressures and purities of the reactants were as follows: *n*-H, 44 Torr (*n*-H, 99.68; 3MP, 0.04; MCP, 0.26); 3MP, 60 Torr (3MP, 99.33; 2MP, 0.61; *n*-H, 0.05); MCP, 41 Torr (MCP, 99.93; *n*-H, 0.07). The temperature of reaction was varied from 523 to 623 K and changed in both an increasing and a decreasing order to detect deactivation. The composition of the reaction mixture after the reactor was determined by sampling on line to a gas chromatograph using a squalane packed column (6 m × ⅛ in.; 80–100 mesh)

RESULTS AND DISCUSSIONS

1. *Characterization of the Parent Ω-Zeolites*

Figure 2 shows the adsorption–desorption isotherms of nitrogen on the samples of Ω-zeolites. The curves exhibit contributions of type I, II, and IV isotherms (*11*). This indicates the presence of microporosity (initial steep rise to a plateau), external surface (departure from the horizontal for the plateau), and mesopores (hysteresis loop). In order to determine the micropore volume *t* or α_s plots are suggested (*12*) for the quantitative treatment of isotherms. We used the latter taking an amorphous silica–alumina material as a reference (Ω-zeolite calcined at 1173 K). The total void volume available for nitrogen was measured from the amount sorbed at a relative pressure $P/P_0 = 0.9$ (in which P is the actual pressure and P_0 the saturation pressure at the temperature of the sample).

The volumes available for *n*-hexane were determined by the uptake of the hydrocarbon at $P/P_0 = 0.2$ (micropore volume) and $P/P_0 = 0.9$ (total volume) as shown elsewhere (*6*).

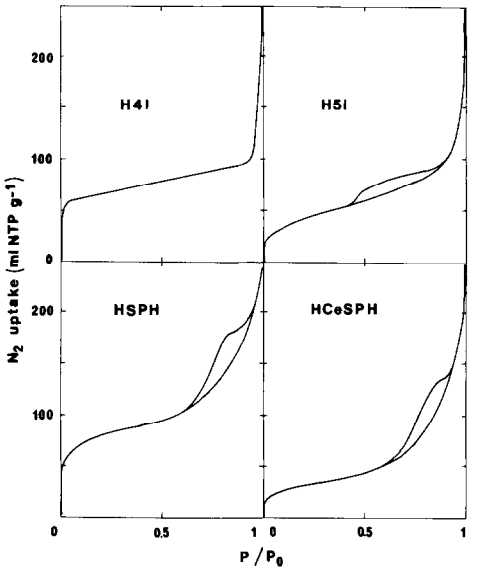

FIG. 2. Adsorption–desorption isotherms for nitrogen at 77 K on HSPH, HCeSPH, H4I, and H5I Ω-zeolites.

Table 1 gives some features of the structural and textural properties of the starting solids calcined at 773 K. The data collected prompt two comments:

(a) For the measurement of specific area in microporous materials the validity of BET formalism is questionable (*12*). Two

TABLE 1

Si/Al Ratios and Sorption Capacities ($cm^3\ g^{-1}$) of the Parent Zeolites Omega

Samples	Si/Al	S_{BET} ($m^2\ g^{-1}$)	Nitrogen uptake[a] P/P_0		*n*-Hexane uptake[b] P/P_0	
			c	0.9	0.2	0.9
HSPH	3.3	290	0.093	0.279	0.04	0.18
HCeSPH	3.4	120	0.027	0.224	0.005	0.18
H5I	2.9	220	0.050	0.110	0.061	0.121
H4I	3.1	210	0.079	0.100	0.077	0.080

Note. [a] At 77 K; [b] at 298 K; P, actual sorbate pressure; P_0, saturation pressure of sorbate at temperature of the sample; [c] micropore volumes were determined by the α_s-plot method.

kinds of phenomenon mislead the interpretation of data: (i) in large micropores (7–18 Å), as in the supercage on Y zeolite, the specific surface may be overestimated due to cooperative adsorption (*12*); (ii) in small micropores (3–7 Å) the specific area may be underestimated due to steric hindrance (*13*). The latter seems to occur for Ω-zeolites since the theoretical value for the specific surface of the main channel (490 m^2 g^{-1}), derived from simple geometrical considerations, is not obtained. Nevertheless, the values quoted in Table 1 can be used for comparative purposes.

(b) When deduced from the theoretical structure of the Ω-zeolite, the pore volume of the main channel is 0.091 cm^3 g^{-1} (*14*). The nitrogen uptake in micropores shows that this value is approached by HSPH and H4I samples. By contrast the spherulitic Ω form HCeSPH develops the smallest microporosity upon cerium exchange. On this sample the void volume is located mainly in mesopores with apertures ranging from 2 to 6 nm as nitrogen desorption showed. H4I and H5I do not exhibit a substantial mesoporosity.

All these samples exhibit a good crystallinity, so the low microporosity of HCeSPH cannot be ascribed to a collapse of the structure. This behavior is better interpreted as a pore blockage by cerium species, which reduced the intracrystalline void volume accessible for nitrogen and especially for *n*-hexane sorption. Consequently the contribution of intracrystalline catalysis will increase according to the sequence HCeSPH < HSPH < H5I < H4I samples.

2. *Preparation of the Bifunctional Pt/Ω-Zeolites Catalysts*

It is obvious, bearing in mind the reactants used in this study, that only a fraction of the void volume of the main channel becomes available to catalysis. Hence it is necessary that the metallic function be located either in this accessible volume or outside the zeolite framework, but not in the gmelinite cage since the reactant cannot enter these cages. In mazzite, the natural analog of Ω-zeolite, divalent cations such as Ca^{2+} and Mg^{2+} prefer the sites of high coordination located in the gmelinite cage (*7*). The exchange of NH_4SPH parent zeolite with cerium was undertaken in order to occupy the gmelinite cage by Ce^{3+} ions and thus prevent the migration of platinum species which might occur during the calcination step. Such a migration takes place from the supercages to the sodalite cages during the calcination of $(Pt(NH_3)_4)$/Y (*15*).

The main characteristics of the platinum/Ω-SPH catalysts are presented in Table 2. In the nomenclature used, the denomination 0.15PtHCe, for instance, refers to a HCeSPH Ω-zeolite containing 0.15 wt% Pt. One of the objectives was the introduction of platinum in a highly dispersed state inside the Ω framework. Actually changing the liquid/solid ratio, the temperature of calcination, in the range 673–823 K, and the nature of the compensation cation has little influence on the dispersion of platinum. The only relevant parameter is the flow rate and the H_2/N_2 ratio during the reduction step, or more precisely the partial pressure of water resulting from the reduction of oxide-like platinum species. When platinum is supported on alumina or faujasite a contact time of 0.5 s^{-1} during the reduction step is sufficiently low to reach H/Pt values close to unity. Under similar conditions for the Pt/Ω-zeolite samples prepared in this work, H/Pt does not exceed 0.40. In order to obtain highly dispersed platinum (H/Pt > 0.9) reduction must be performed under a high flow rate of diluted hydrogen. When this condition is respected, liquid/solid ratio, calcination temperature, and cerium exchange have little influence, as samples V, X, and XI show. It is well established now that water favors the sintering of metal crystallites. Thus the different behaviors for platinum reduction among Pt/alumina, Pt/faujasite, and Pt/Ω-zeolite probably arise from a higher water pressure in the

TABLE 2

Main Features of the Catalysts (SPH Samples)

Sample		S_{BET} ($m^2\ g^{-1}$)	H/Pt	S_{Pt} ($m^2\ g^{-1}$ cat)	Mean particle size (nm)	Crystallinity[c] (%)
Name	Number					
0.18PtH[a]	I	210	0.37	0.20	2.6	65
0.43PtH[a]	II	224	0.45	0.57	2.1	35
0.81PtH[a]	III	—	0.30	0.73	3.0	26
1.56PtH[a]	IV	62	0.20	0.98	5.0	10
0.26PtH[b]	V	190	>1	0.78	1.0	72
0.17PtH[a]	VI	260	0.4	0.20	2.5	72
0.08PtHCe[a]	VII	110	0.38	0.09	2.5	100
0.15PtHCe[a]	VIII	—	0.37	0.17	2.6	95
0.37PtHCe[a]	IX	64	0.18	0.20	5.2	93
0.19PtHCe[b]	X	106	0.75	0.43	1.4	88
0.17PtHCe[b]	XI	100	0.90	0.46	1.1	58

[a] H_2 flow rate in the reduction step: 2 $cm^3\ s^{-1}$.
[b] $H_2 + N_2$ (80 + 20%) flow rate in the reduction step: 5 $cm^3\ s^{-1}$.
[c] Referring to the NH_4SPH or NH_4CeSPH zeolite.

latter solid, probably due to diffusional limitations: during the reduction step the removal of water outside the Ω framework is low not only from the gmelinite cage but also from the main channel.

One can see that the introduction of cerium modifies little the dispersion of platinum. However, with the Ce-exchanged zeolite the increase in platinum content is less detrimental with respect to the crystallinity and surface area. Indeed, large platinum particles in the 5 nm range are obtained, but at lower Pt loadings. Since the aperture of the main channel does not exceed 0.8 nm, the location of such large particles needs to be considered. Are these particles outside the zeolite structure or occluded inside, as reported for RuY catalysts (*16*)? The catalytic data may clarify this point.

3. *Conversion of Alkanes over Pt/Ω-Zeolite Catalysts*

We studied the hydroconversion of *n*-hexane, 3-methylpentane, and methylcyclopentane on Pt/Ω catalysts of various metal loadings, i.e., different metallic surfaces ranging from 0.1 to 1 m^2 per gram of catalyst (Fig. 3). From the first review by Minachev and Isakov (*17*) to the extensive study by Guisnet and Perot (*18*) it is well established that activity and selectivity in alkane hydroconversion on a bifunctional catalyst depend on the balance between the hydrogenating and the acidic functions. The activity is proportional to the metallic surface at low metal content and then

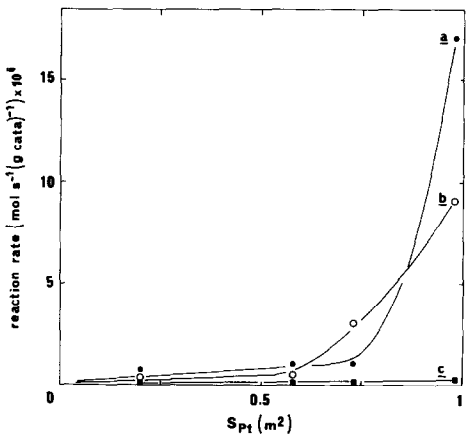

FIG. 3. Rate [mol s^{-1} (g cat)$^{-1}$ × 10^6] of alkane hydroconversion as a function of the platinum surface in Pt/HSPH catalysts; (a) *n*-hexane, (b) 3-methylpentane, (c) methylcyclopentane. Reaction temperature, 583 K; conversion, 2.5%.

TABLE 3

Conversion of *n*-Hexane in the Presence of Hydrogen over Pt/Al_2O_3 Catalyst at 583 K (Total Conversion 3.5%)

Rate (mol s^{-1} (g cat)$^{-1}$)	Hydrogenolysis		Isomerization	
	Selectivity (%)	E_a (kcal mol^{-1})	Selectivity (%)	E_a (kcal mol^{-1})
$3.8\ 10^{-7}$	78.5	28.3 ± 1.2	20.2	45.8 ± 2.6

reaches a plateau around 0.5 wt% Pt for zeolites mordenite and Y (*18*). This plateau is attained for a metallic surface around 0.5–1 m^2 (g cat)$^{-1}$. When the acidic function is not sufficiently balanced the selectivity for cracking products increases.

First, the specific properties of platinum have been estimated with the Pt/alumina sample, used in mechanical mixtures. Table 3 reports the overall activity and selectivities at 583 K, and the activation energies for *n*-hexane conversion. From these data the conversion due to platinum alone, in the mechanical mixtures, can be determined and subtracted from the overall rate, to estimate the importance of purely acid-catalyzed reactions on Pt/Ω-zeolite catalysts.

During the hydroconversion of *n*-hexane, Ω-zeolite samples without platinum suffer a strong deactivation, so no relevant information can be recorded from these experiments. In mechanical mixtures, composed of Ω-zeolite with Pt/Al_2O_3, HSPH deactivates substantially, while the activity of HCeSPH does not decline. Actually the introduction of platinum greatly stabilizes the catalytic activity even though samples I and VII with the lowest metallic surface suffer a 60% decrease in activity, while for sample IV only a 2% decrease is observed. For all the catalysts the reaction rate falls when increasing the contact time, even at very low conversion levels on some catalysts (conversion level <2%). Obviously this last observation discards any thermodynamic limitation and suggests diffusional problems. The fact that this behavior takes place at higher conversions on mechanical mixtures and samples IV and IX calls for two comments: (i) the sharp decrease in activity on increasing the contact time probably arises from the presence of platinum particles in the zeolite framework which slow down the diffusion of reactant; (ii) the similar behaviors of catalysts IV and IX and of the mechanical mixtures suggest a hydrogenating function located outside the Ω structure in the former; this last point would be in line with the large size of the platinum particles (>5 nm). These two ideas are strengthened by the catalytic properties reported in Tables 4 and 5.

It should be noted that the intrinsic activity of the metallic function, for hydrogenolysis and isomerization, is not recovered, probably due to a fast initial poisoning of the platinum surface. On the acidic sites isomerization leads to 2MP or 3MP from *n*-H and to cyclohexane by ring enlargement from MCP; by β-scission of secondary carbocations cracking gives propane from *n*-H (through 2MP), and *n*-H from MCP ring opening. Thus two distinct behaviors can be separated: (i) On samples presenting large platinum particles (>5 nm) and on the mechanical mixture with HCeSPH, the specific activity per square meter of metallic surface is high, and the selectivity for isomerization is large. The activation energies are close to those previously found with "ideal hydroisomerization" catalysts (*19, 20*). (ii) On catalysts with small or medium platinum particles ($d < 5$ nm) the specific activity is low, with respect to the Pt surface area, the selectivity to cracked products increases, and the activation energies decrease. It must be noted that this phenomenon occurs at conversion levels as small as 1–2% and is enhanced for MCP, the more hindered molecule. Some of the activation energies approach values characteristic of a diffusional mass transport (5–10 kcal mol^{-1}).

These facts can be interpreted assuming that on the samples where the platinum particles are smaller than 5 nm, they are lo-

TABLE 4

Activation Energies and Reaction Rates at the Steady State, at 583 K of C_6 Hydrocarbon Conversions in the Presence of Hydrogen over Platinum/Ω-Zeolite Catalysts (SPH Samples)

Samples		Transformation rate (mol s^{-1} (g zeol)$^{-1}$) × 10^7			Activation energy (kcal mol^{-1})		
Name	Number	*n*-H	3MP	MCP	*n*-H[a]	3MP[a]	MCP[b]
0.18PtH	I	3.4	7.7	1.5	—	—	—
0.43PtH	II	4.5	11	0.6	21.5	15.5	9.7
0.81PtH	III	30	15	0.4	32.5	—	—
1.56PtH	IV	91	170	2.2	38.0	21.5	—
0.26PtH	V	2	48	1.3	25	14.0	18.0
0.17PtH	VI	5	6	1.3	16.5	15.0	16.5
0.08PtHCe	VII	0.37	10	0.37	13	13	7
0.15PtHCe	VIII	1.3	20	—	19	14	—
0.37PtHCe	IX	9.2	21	0.67	37	26.5	36
0.19PtHCe	X	3	70	1.2	19	19	16
0.17PtHCe	XI	1	16	0.66	20.5	20	17.5
Pt + HCeSPH[c]		5.4	26	2.7	35	26.5	28
Pt + HSPH[c]		4.2	—	1	34	—	27

[a] Determined at 2.5% conversion.

[b] Determined at 1% conversion.

[c] Composition, Ω-zeolite–Pt/Al_2O_3 (90–10 wt%); platinum surface = 0.1 m^2 (g cat)$^{-1}$.

TABLE 5

Selectivity Pattern in *n*-Hexane and Methylcyclopentane Conversion at 583 K over Platinum/Ω-Zeolite Catalysts (Conversion between 1 and 3%)

Sample		*n*-Hexane			Methylcyclopentane	
Name	Number	Cracking		Isomerization	Ring opening	Ring enlargement
		Metallic[a]	Acid			
0.18PtH	I	—	3.8	96.2	46	53
0.43PtH	II	—	8.3	91.7	36.3	59.1
0.81PtH	III	—	5.2	94.8	21.6	76.3
1.56PtH	IV	1.0	—	100	14.2	85.8
0.26PtH	V	—	20.6	79.4	48.4	49.2
0.17PtH	VI	—	12.7	87.3	22.4	75.2
0.08PtHCe	VII	—	17	83	63.2	29.8
0.15PtHCe	VIII	—	10.6	89.4	—	—
0.37PtHCe	IX	—	0.5	99.5	6.6	88.3
0.19PtHCe	X	—	17.5	82.5	49	47.8
0.17PtHCe	XI	—	20	80	38.7	54.2
Pt + HCeSPH		2.0	—	100	15	85
Pt + HSPH		1.0	15	85	23.5	74

[a] Determined from the C_1 and C_2 fractions in light products.

cated inside the Ω structure and hinder strongly the diffusion of the reactants. The understanding of catalytic properties is then straightforward. When platinum particles are inside the framework of the zeolite the activity is not directly proportional to the platinum surface for two reasons (Fig. 3): the metallic particles slow down the transport of reactant, and some of them are not available for catalysis. The former explains the decrease in the activation energy.

When diffusional limitations occur the increased selectivity into cracked products may be interpreted by two linked phenomena: the reactant partial pressure would be lower within the particles of the zeolite and the real contact time could be larger than the apparent one. Thus the conversion level inside the pores would be larger than that recorded at the reactor outlet. Probably inside the pores of the zeolite the distribution of the isomerization products (2MP, 3MP for *n*-H conversion) is close to the thermodynamic equilibrium, and secondary reaction by β-scission becomes noticeable.

These results allow us to postulate some ideas about the location of platinum in these Pt/Ω-zeolite catalysts: (i) platinum particles smaller than 1 nm are located in the main channel, and probably in the gmelinite cages or the secondary channels too, since all of the platinum surface is not accessible for the reactants; (ii) when the size of the platinum particles increases to 3–4 nm the particles stay inside the zeolite structure by creating cavities in the core of the framework; (iii) for the larger metallic particles of samples IV and IX (>5 nm) the platinum is located outside the framework.

In this last case, most of the metallic surface becomes available, and these catalysts behave like a mechanical mixture. One can note that a severe crystal collapse of the zeolite occurs for the HSPH-based catalyst but not for the HCeSPH-based one, as evidenced by the decreases in specific area and crystallinity (Table 2). We think that during crystal growth of Pt, particles initially located inside the main channel can migrate outside it, thereby preventing destruction of the structure. This migration is hindered for platinum species located in the gmelinite cage, so the growth of these particles leads to a collapse of the zeolite. As previously suggested, a preexchange with cerium would prevent this phenomenon.

With the parent zeolite used, even when a well-dispersed Pt/Ω-zeolite is prepared (sample V), the catalyst obtained suffers strong diffusional limitations and the catalytic properties are not related to the acidic properties of the solid. Therefore the mechanical mixtures are a useful tool for the investigation of the properties of the zeolite. Table 6 presents the catalytic behavior of mechanical mixtures of H4I and H5I zeolites with Pt/alumina. Like the HSPH sample, H4I and H5I differ noticeably from HCeSPH Ω on three points: first, the selectivity for cracking is high, even at low conversion; second, specific activities differ by one order of magnitude; and third, the ini-

TABLE 6

Catalytic Properties of Mechanical Mixtures Composed of Ω-Zeolite H5I and H4I with Pt/Al_2O_3 in the Hydroconversion of *n*-Hexane and Methylcyclopentane at 583 K

Sample	*n*-Hexane				Methylcyclopentane		
	Rate (mol s^{-1} g^{-1} zeol)	$S_{isom.}$ (%)	$S_{crack.}$ (%)	E_a (kcal mol^{-1})	Rate (mol s^{-1} g^{-1} zeol)	Ring enlargement (%)	Ring opening (%)
Pt + H5I	2.2×10^{-7}	90	10	31.5	2.1×10^{-7}	34.8	62
Pt + H4I	8.5×10^{-8}	85	15	33.5	4.2×10^{-8}	42	52

tial deactivation is more pronounced, being 5% for HCeSPH, but 30% for H5I, and more than 70% for H4I. However, only small differences appear between the activation energies. With respect to *n*-hexane it can be concluded that little pore blockage exists for the different catalysts. Moreover, on HCeSPH intercrystalline catalysis will prevail (*n*-hexane uptake = 0.005 $cm^3 g^{-1}$ at $P/P_0 = 0.2$), the reverse being true for HSPH, H4I, and H5I zeolites. Therefore the large difference in selectivity between HCeSPH and the latter can be understood by the distance separating the hydrogenating and the acidic functions. Before hydrogenation at the platinum surface the olefins suffer degradation reactions, the extent of which depends on the diffusional path length. The slight change of selectivity among HSPH, H4I, and H5I zeolites may arise from differences in micropore void volume or from different mean lengths of the zeolite crystals (0.2 μm for H5I and H5PH, 2 μm for H4I). A more detailed study of the selectivity pattern in *n*-H conversion on H4I, at short time on stream, shows that C_4 and C_5 alkanes represent 70% of the cracked products. The presence of *i*-C_4, *n*-C_4, *n*-C_5, and *i*-C_5 points out the importance of secondary reactions between olefins and carbocations. As stated previously, *n*-C_4 and *n*-C_5 do not come from *n*-H hydrogenolysis over platinum owing to the absence of ethane and methane in the effluents.

In conclusion, highly dispersed platinum/Ω-zeolite catalysts have been prepared with metallic particle sizes as small as 1 nm. The conditions of preparation of such a material are more delicate than with other zeolites. Part of the platinum particles probably located in the gmelinite cages are not available for catalysis; therefore, an initial exchange with cerium is advantageous by impeding the access of precursors of platinum particles to these cages. This study emphasizes the importance of diffusional problems in the Ω-zeolites investigated. A slow diffusion of water during the reduction of oxide-like platinum species induces sintering by increasing the partial vapor pressure inside the crystal lattice. During catalysis the diffusion of reactants is hindered by small particles of platinum. The influence of the length of the crystals in the *c*(001) direction on the catalytic properties of H4I and H5I Ω-zeolite may be rationalized in the same way. This general behavior of Ω-zeolite arises from the tubular unidimensional character of this zeolite, since the transport of reactants and products takes place only along the *c* direction in the 12-membered ring of the main channel.

ACKNOWLEDGMENTS

The authors gratefully thank Dr. François Fajula for helpful discussions, and the Service Central d'Analyse (CNRS) for chemical analysis of the samples.

REFERENCES

1. Cole, J. F., and Kouwenhoven H. W., *ACS Adv. Chem. Ser.* **121,** 583 (1973).
2. Perrotta, A. J., Kibby, C., Mitchell, B. R., and Tucci, E. R., *J. Catal.* **55,** 240 (1978).
3. Solinas, V., Monaci, R., Marongiu, B., and Forni, L., *Appl. Catal.* **5,** 171 (1983).
4. Fajula, F., Ibarra, R., Figueras, F., and Gueguen, C., *J. Catal.* **89,** 64 (1984).
5. Flanigen, E. M., French Patent 1,548,382 (1968).
6. Chauvin, B., Fajula, F., Figueras, F., Gueguen, C., and Bousquet, J., *J. Catal.* **111,** 94 (1988).
7. Galli, E., *Cryst. Struct. Commun.* **3,** 339 (1974).
8. Fajula, F., Figueras, F., Moudafi, L., Vera Pacheco, M., Nicolas, S., Dufresone, P., and Gueguen, C., French Patent Appl. 850772 (1985).
9. Vera Pacheco, M., Ph.D. thesis, Montpellier, 1985.
10. Ribeiro, F., and Marcilly, C., *Rev. Inst. Fr. Pet.* **34,** 405 (1979).
11. Brunauer, S., Deming, L. S., Deming, W. S., and Teller, E., *J. Amer. Chem. Soc.* **62,** 1723 (1940).
12. Gregg, S. J., and Sing, K. S. W., "Adsorption, Surface Area and Porosity," 2nd ed. Academic Press, London/New York, 1982.
13. Bonnetain L., and Ginoux, J. L., private communication, 2nd meeting "Groupe Français des Zéolithes," Mulhouse, 1986.
14. Breck, D. W., and Grose, R. W., *ACS Adv. Chem. Ser.* **121,** 319 (1973).
15. Gallezot, P., *in* "Catalysis by Zeolites" (B. Imelik, C. Naccache, Y. Ben Taarit, J. C., Védrine, G. Coudurier, and H. Praliaud, Eds.), p. 227. Elsevier, Amsterdam, 1980.

16. Verdonck, J., Jacobs, P. A., Genet, M., and Poncelet, G., *J. Chem. Soc. Faraday Trans. 1*, **74,** 403 (1980).
17. Minachev, Kh. M., and Isakov, Ya. I., *in* "Zeolite Chemistry and Catalysis" (J. A. Rabo, Ed.), p. 552, ACS Monograph 171. Amer. Chem. Soc., Washington, DC, 1976.
18. Guisnet, M., and Perot, G., *in* "Zeolites: Science and Technology" (F. R. Ribeiro, A. E. Rodrigues, L. D. Rollman, and C. Naccache, Eds.), p. 397. Nijhoff, The Hague, 1984.
19. Chick, D. J., Katzer, J. R., and Gates, B. C., *in* "Molecular Sieves II" (J. R. Katzer, Ed.), p. 515, ACS Symposium Series 40. Amer. Chem. Soc., Washington, DC, 1977.
20. Ribeiro, F., Marcilly, C., and Guisnet, M., *J. Catal.* **78,** 267 (1982).